DOI: 10.47743/achi-2025-2-0008 *ACTA CHEMICA IASI*, **33_2**, 143-166 (2025)

BEYOND THE AROMATIC AMINO ACID VIOLET-BLUE FLUORESCENCE: A SPECTROSCOPIC AND OPTICAL MICROSCOPY STUDY

Teodora Culiță[a], Florin Bucatariu[b] and Vasile-Robert Grădinaru[a*]

[a]*Department of Chemistry, "Al.I. Cuza" University Iasi, 11 Carol I Bd Iasi 700506, Romania*

[b]*Petru Poni Institute of Macromolecular Chemistry, 41A Grigore Ghica Voda Alley, 700487 Iasi, Romania*

Abstract: Given that high levels of aromatic amino acids in the human body can lead to cognitive impairment, IQ deficit and neurological function, their self-assembly process should be deeply investigated as function of their concentration. This study highlighted that 2D and 3D fluorescence spectroscopy is a useful technique that can be used to study self-assembly of aromatic amino acids at physiological concentrations and higher incubation times. Overall, our experimental 2D data clearly supports that blue fluorescence is a result of phenylalanine and tyrosine self-assembly and not to tryptophan when concentration of 100 µM of each amino acids were incubated over days times periods. Phenylalanine behavior in solutions was assessed at 100 and 200 µM by 3D fluorescent analysis. The blue fluorescent signal at around 443 nm could be assessed using 225 or 315 nm excitation wavelengths. The self-assembly was monitored at concentration of 1 mM phenylalanine which matches that one in phenylketonuria. At higher intensity a violet fluorescence was observed at an excitation of 315 nm. The emission maximum was shifted from 398 nm (after 48 h) to 444 nm (more than three days). Based on intrinsic violet-blue fluorescence of supramolecular complexes or conventional microscopical techniques, the outcomes of this work are crucial for determining the self-assembly capability of more complicated molecules, such as peptide and proteins.

***Keywords*:** aromatic amino acids; spectrophotometry; violet-blue fluorescence; optical microscopy

*Vasile Robert, Gradinaru, *e-mail:* robert.gradinaru@uaic.ro

Introduction

Aromatic amino acids distinguish by their properties to absorb UV light in both UVC and UVB domain.[1] This property are valuable in order to study their behavior in aqueous solutions that are mimicking the normal physiological conditions or to monitor the protein concentration during chromatographic separation or fractionation based on the presence of aromatic moieties.[2] Therefore, fluorescence spectroscopy is a more suitable technique that allows a high sensitivity, compared to classical UV spectroscopy. The aromatic amino acids, phenylalanine (Phe), tyrosine (Tyr) and tryptophane (Trp) are able to emit light when are excited bellow 280 nm (257 nm for Phe, 274 for Tyr and 280 nm for Trp).[3] The calculated UV and fluorescence spectra of Tyr, Trp and Phe are comparable with experimental data.[4] Intrinsic fluorescence of aromatic amino acids could be exploited in studying their capacity to self-organize in solution. 3D fluorescence spectra are a collection of emission spectra obtained at different excitation wavelengths using a constant scanning speed. 3D fluorescence fingerprinting is an appropriate technique for recognition, classification or food processes monitoring.[5] Usually, a fluorescence landscape map is obtained, and each relevant fluorophore has a specific fingerprint. Due to these properties complex samples containing multiple fluorophores or aggregation phenomena could be investigated.[6]

Some inherited disorders are characterized by single amino acid type accumulation. Thus, a high phenylalanine content is usually observed in patients with phenylketonuria. In these patients' cognitive impairment and neurological functions alteration was found depending on amino acid levels.[7] Another study suggested that in children with phenylketonuria selective impairments in executive functioning were noticed according to

their phenylalanine concentration.[8] There is also an evident association between high blood phenylalanine levels and poor mood / sustained attention of adult patients having phenylketonuria when compared them with the placebo supplementation.[9,10]

Phenylalanine self-assembles into toxic fibrils might trigger protein aggregation in subjects with phenylketonuria.[11,12] Analogously, tyrosinemia type I, another rare metabolic disease, it is manifested by an elevated tyrosine plasma level and finally affect dopamine content.[13,14] Supplementary, an elevated blood tryptophan (Trp) level was registered in Hartnup disease and hypertryptophanemia.[15,16] Accumulation of tryptophan and its corresponding metabolites might cause brain injuries and can be related to inflammation and neurodegenerative diseases.[17,18] In brief, several diseases are associated with tendency of phenylalanine, tyrosine or tryptophan accumulations which turn on serious diseases. Therefore, hierarchical organizational capacity of aromatic amino acids should be deeply investigated. An earlier study has demonstrated the effect of ionization and concentration on the self-assembly capacity of L-phenylalanine.[19] Zinc assisted self-assembling of phenylalanine into needle-like crystals was also reported. The resulting supramolecular structures display the capacity to assist ester hydrolysis.[20] Similarly, well-ordered supramolecular assemblies of tyrosine were visualized by TEM, AFM, and SEM.[21] Researchers also developed antibodies that allowed detection of these tyrosine fibrils in order to localize these assemblies.[22] Tyrosine dimer assemblies proved to be the basic unit of tyrosine nanotubes. These dimers display photoluminescence properties, with emission in the visible region, when they are suspended or are deposited.[23] A different self-assembling mechanism was reported for tyrosine as compared to

phenylalanine. The phenolic (-OH) and carboxylic (−COOH) groups of tyrosine, and amino ($–NH_2$) groups of phenylalanine are mostly involved in H-bond formation while carboxylate ($−COO^−$) and ammonium ($−NH_3^+$) groups are involved in attractive electrostatic interactions.[24] Tryptophan might undergo a self-assembly process yielding amyloid like nanofibers with relevant toxic effects on neuroblastoma cells.[25] Tryptophan or tyrosine self-assembly in aqueous solution (500 μM) as nanotubes. These supramolecular structures were characterized by FTIR and two different microscopy techniques.[26] Surface-enhanced Raman spectroscopy was also employed to self-assembling of tryptophan monomers into amyloid-like structures. That study provides novel insides on self-assembling of tryptophan by an array of π- π stacking interactions, hydrogen bonding and changes in hydrophobicity.[27]

In this work, we will demonstrate that both fluorescence spectroscopy and microscopy could be used to assess the self-assembly of aromatic amino acids. The mechanism of self-assembly is dictated by type of amino acid used and its concentration. This study focused mainly on phenylalanine and tyrosine as model aromatic amino acids and demonstrates that self-assembly could be assessed in violet-blue emission region or followed by microscopy.

Results and Discussion

The UV-visible spectra of three aromatic amino acids recorded in Tris buffer (0.1 M, pH = 7.4) are displayed in Figure 1. The absorption maxima were 258 nm for phenylalanine, 275 nm for tyrosine and 280 nm for tryptophan when a Tris 0.1 M solution (pH = 7.4), was used. Besides, the absorption spectrum of phenylalanine displays two shoulders at 251 nm

and 265 nm. Tryptophane spectrum contains two additional shoulders at 272 and 289 nm, while tyrosine has just one shoulder at around 281 nm. As expected, the maxima and the spectral fingerprint of each amino acid are in the frame with previously reported data.[28]

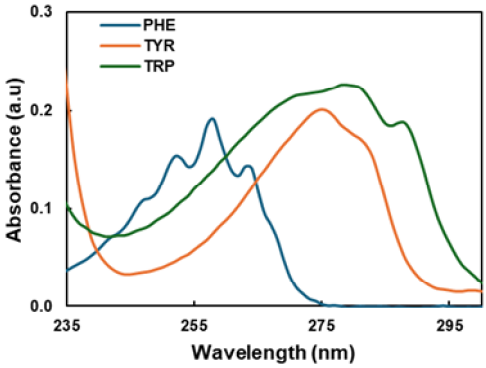

Figure 1. UV-Vis spectra of phenylalanine (1.05 mM PHE; blue), tyrosine (136.3 μM TYR; orange) and tryptophan (35 μM TRP; green) in Tris 0.1 M, pH = 7.4.

The fluorescence spectra of three aromatic amino acids are ilustrated in Figure 2. The emission maxima of phenylalanine was at observed at 282 nm. Tyrosine and tryptophan display strong emission signals at 303 nm and 354 nm at concentration lower than 10 μM. Interestingly, after incubation of phenylalanine for 110 h at 37 degrees the emission maximum was at almost half of initial intensity value and red shifted with 15 nm. In the spectrum two small intensity signals having broad bands at 446 and 528 nm were distinguished. Surprisingly, when a fluorescence spectrum of diluted tyrosine and tryptophan incubated were recorded no emission was observed. The incubated undiluted amino acid stock solutions (100 μM) display a noticeable emission spectrum (Figure 2). For tyrosine a similar pattern to phenylalanine with an emission signal of 514 arbitrary units (a.u.) at 443 nm was noticed. However, the signal from 303 nm was drastically

decayed and a red shift to 321 nm (and intensity 631 a.u.) was observed. The tryptophan behaves differently, and its maximum was blue shifted to 334 nm (intensity 844 a.u.). Most probably the presence of indolyl moiety could induce a different array of noncovalent interaction due to the supplementary H bonds that are involved in intermolecular interaction.[29] Molecular dynamic simulation were also performed to study aromatic amino acids self-assembly. Hydrophobic and polarity effects seems to have an impact on the kinetics of assembly processes and the supramolecular assemblies that arise. Tryptophan molecules have a unique structural characteristic imprinted by the indole side chain.[30]

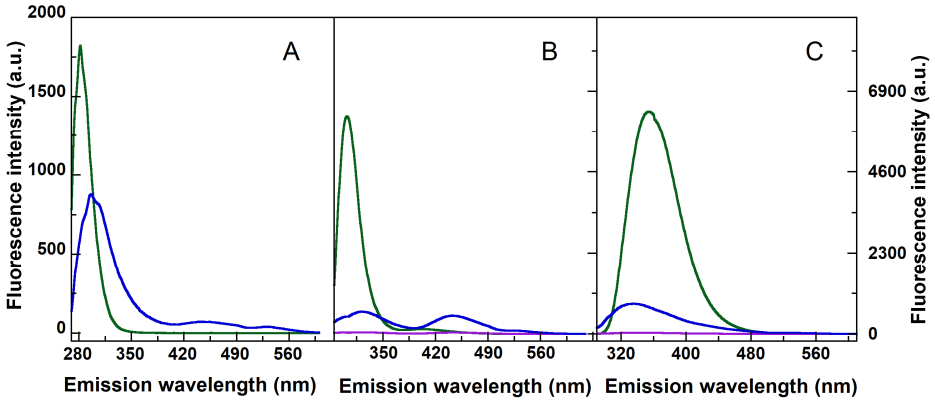

Figure 2. Emission spectra of three aromatic amino acids. *Panel A:* Phenylalanine 100 µM before (green) and after incubation at 37 degrees for 110 h; *Panel B:* Tyrosine 8 µM before (green) and after incubation (8 µM – magenta; 100 µM –blue) at 37 degrees for 111 h; *Panel C:* Tryptophan 5.25 µM before (green) and after incubation (5.25 µM – magenta; 100 µM –blue) at 37 degrees for 112 h. Conditions: Tris 0.1 M, pH = 7.4.

The above fluorescence data clearly suggested that a blue fluorescence is observed for both phenylalanine and tyrosine when samples were incubated more than 110 h. Supplementary, a new test was performed and the decay of emission at 303 nm was followed at various incubation times. Thus, the incubated tyrosine sample (100 µM) was diluted (1:12.5) in the same buffer and each spectrum was recorded in the same emission wave

range (Figure 3). At 46 h incubation a small intensity emission peak was noticed, and the maximum was red shifted to 327 nm, at longer incubation time (146 h) the emission signals were almost abolished. These data were in the frame with the experimental data presented in Figure 2 (Panel B).

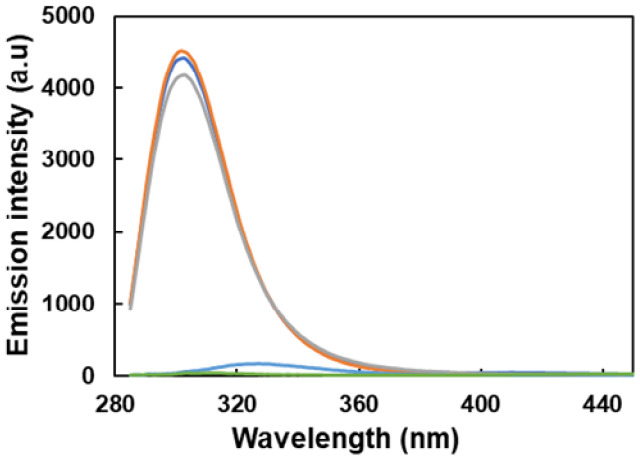

Figure 3. 2D emission spectra of diluted tyrosine (8 μM) prepared in 50 mM Tris buffer at pH 7.4. The spectra were recorded initially (dark blue), at 1 h (orange), 25.5 h (gray), 46 h (light blue), and 146 h (green) as a function of incubation time at 37 degrees using a 100 μM stock solution.

It is known that plasma concentration of phenylalanine range in 39 – 85 μM in adults and slightly higher in children 130 μM.[31,32] However, in hyperphenylalaninemia the amino acid concentration is situate in a range of 120-599 μM and in phenylketonuria blood level might reach 1200 μM (mild form) or higher (classical case).[33] Different morphologies were observed when self-assembly of phenylalanine at higher amino acid concentrations was investigated.[19]

In this study we have focused on spectral changes using normal (100 μM) or slightly higher (200 μM) phenylalanine concentration. Firstly, we follow the 3D phenylalanine emission profiles at a low concentration. Initially, two intense peaks centered at 217 nm/282 nm and 257 nm/282 nm

were noticed (Figure 4, Panel A and Table 1). The emission pattern was slightly similar after 16 h of incubation (Figure 4, Panel B). The profile was different when a longer incubation (37 h, Figure 4, Panel C) was performed, and two spectral shadows have been extended to the visible emission domain. Finally, when amino acid sample was incubated 61 h the emission spectra revealed two signals centered at 227.0/444.0 respectively 315.0/445.5 (ex/em). Obviously, this blue emission (Figure 4, Panel D) at around 445 nm arises and probably might be attributed to some well-organized structures resulted by self-assembly. A similar pattern was noticed after 162 h of incubation (Figure 4, Panel E), but these centered signals had vanished after 264 h (Figure 4, Panel F).

A recent study by Bagchi and colab. has demonstrated that these intrinsic blue emission properties are a consequence of both nanoparticles and fibrils formation. This "clusteroluminescence" is also triggered by Na^{+}, Mg^{2+} and Ca^{2+} when fibrils are formed or by Zn^{2+}, Al^{3+} respectively Ga^{3+} when nanoaggregates are observed.[34] However, high aromatic amino acids concentrations (20 mM) were used which are far away from physiological or pathological values. Nevertheless, our buffer (Tris) contains a primary amine-based compound, 2-Amino-2-(hydroxymethyl)-1,3-propanediol, having a pKa of 8.3. Thus, at pH 7.4 this molecule is partially positive and plays a definitory role in self-assembling process. Aromatic amino acids have an isoelectric point (pI) situated in a range of 5.6-5.9. Tyrosine displays an isoelectric point of 5.63, phenylalanine has an pI of 5.76 and tryptophane a value of 5.88 for its pI.[35] Therefore, in our experimental condition all amino acids are mainly negatively charged. In this respect, electrostatic intramolecular interactions are also involved in self-assembling process.

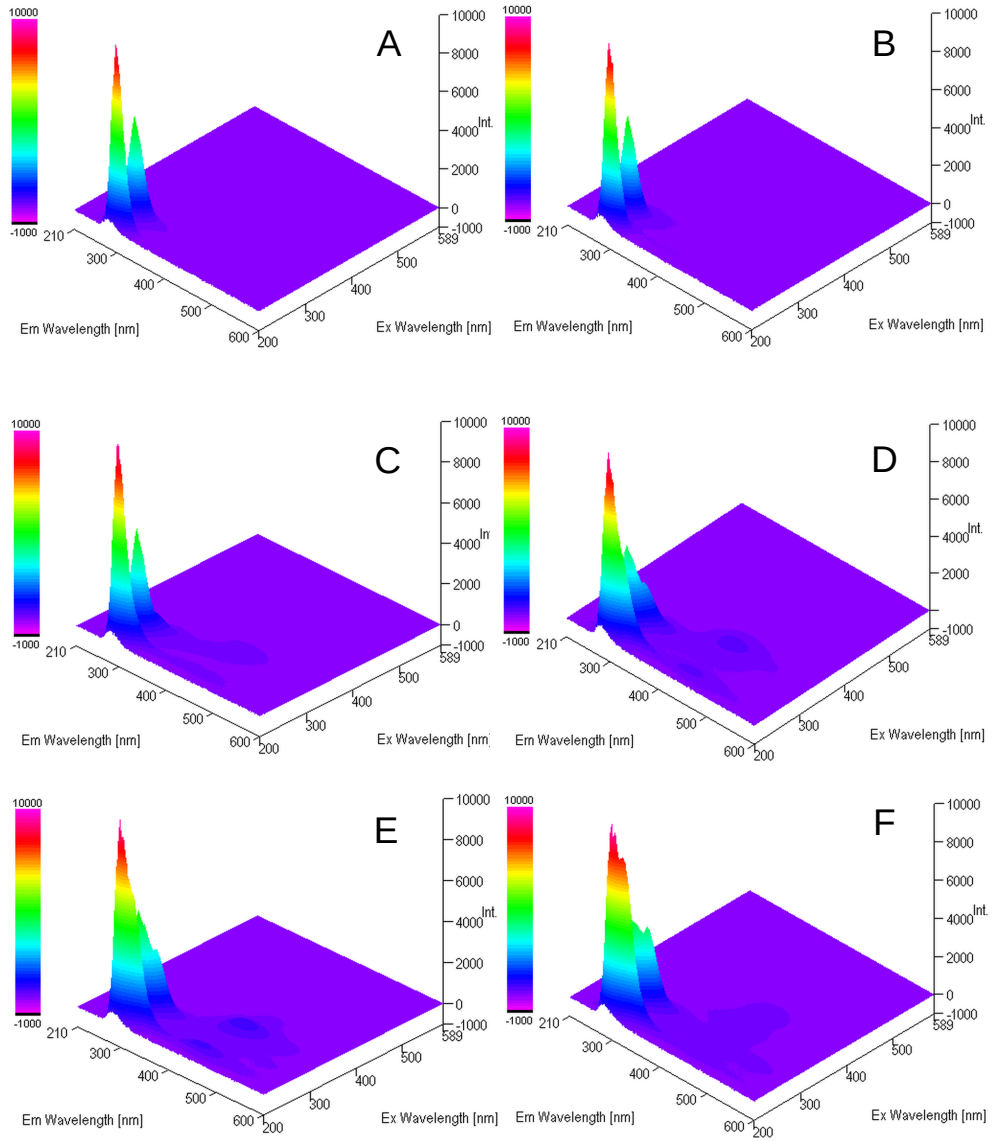

Figure 4. 3D Emission spectra of phenylalanine (100 µM) in 50 mM Tris buffer at pH 7.4 before and after incubation at 37 degrees. The spectra were recorded immediately (Panel A), at 16 h (Panel B), 37 h (Panel C), 61 h (Panel D), 162 h (Panel E) and 264 h (Panel F).

Secondly, a similar set of experiments was performed in order to follow the 3D emission patterns at a concentration phenylalanine of 200 µM. In this case the profile was slightly different, having a dominant

emission peak centered at 257.0 nm/279.5 nm. Our result is in frame with a study of tyrosine, tryptophane and human serum albumin where the second peak was attributed to the presence of aromatic residues.[36]

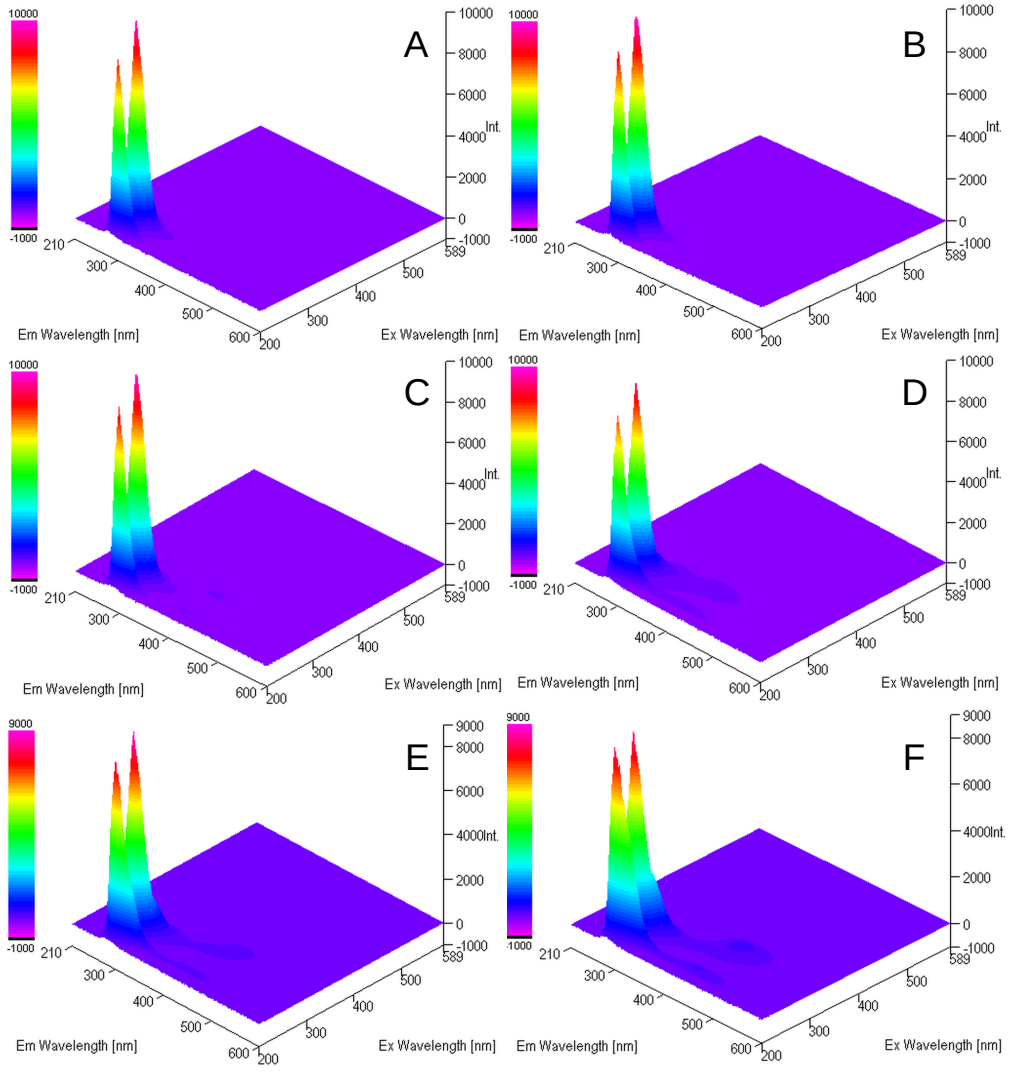

Figure 5. 3D Emission spectra of phenylalanine (200 µM) in 50 mM Tris buffer at pH 7.4 before and after incubation at 37 degrees. The spectra were recorded immediately (Panel A), at 1 h (Panel B), 13 h (Panel C), 25 h (Panel D), 40 h (Panel E) and 64 h (Panel F).

The profiles were almost identical for initial and 1h incubated samples (Figure 5, Panel A and B). After 13 h of incubation two faded spots (ex/em 224.0 nm/443.5 nm and 313.0 nm/440.5 nm; Table 2) were observed (Figure 5, Panel C), then a similar trend was noticed as that one displayed in Figure 4. As expected, the resulting signals were more evident at short incubation times and higher phenylalanine concentration. However, initially the signal I_4 (Table 2) is modest compared with I_3, but later at incubation times that exceed 60 h the signals display similar intensities.

Table 1. The recorded emission intensities of phenylalanine peaks at their corresponding excitation (nm) / emission (nm) pairs in UV range.

Concentration (μM)	**Incubation time (h)**	**Ex_1 /Em_1**	**I_1 (a.u.)**	**Ex_2 /Em_2**	**I_2 (a.u.)**
100	0	217.0/282.5	9161	257.0/282.0	5033
	16	216.0/281.5	9402	257.0/281.5	4954
	37	216.0/281.5	9646	257.0/282.0	5006
	61	216.0/282.0	9828	257.0/281.0	4088
200	0	219.0/282.5	8322	257.0/281.5	9762
	1	219.0/282.5	8770	257.0/279.5	9856
	13	219.0/282.0	8783	257.0/280.5	9804
	25	219.0/281.0	8025	257.0/281.5	9201
	40	218.0/282.5	8032	257.0/282.5	8955
	64	219.0/282.0	8297	257.0/281.5	8523

Table 2. The recorded emission intensities of phenylalanine peaks at their corresponding excitation (nm) / emission (nm) pairs with emission in visible range.

Concentration (μM)	Incubation time (h)	Ex_3 /Em_3	I_3 (a.u.)	Ex_4 /Em_4	I_4 (a.u.)
100	0	226.0/443.5	4.7[d]	318.0/448.0	d
	16	225.0/444.5	47.7	314.0/439.5	9.0
	37	225.0/445.0	136.8	315.0/448.0	93.0
	61	227.0/444.0	317.0	315.0/445.5	301.5
200	0	226.0/448.5	1.4[d]	d	d
	1	224.0/444.0	23.4	313.0/443.5	7.2
	13	224.0/443.5	40.0	313.0/440.5	14.9
	25	226.0/443.0	61.2	294.0/438.0	68.5
	40	226.0/443.0	165.5	318.0/442.5	137.4
	64	225.0/441.0	308.7	319.0/443.0	316.4

d – difficult to be quantified

Lastly, a dynamic assay was performed at higher phenylalanine concentration (1 mM) and 37 degrees. Each 2D emission spectrum was taken in the range of 325-600 nm using an excitation wavelength of 315 nm. The emission intensity at 406 nm was slowly increasing with incubation time. It should be emphasized that violet fluorescent signal was modest in the first ten incubation hours (less than 25 a.u; Figure 6). This emission intensity was almost equivalent to that one recorded for incubation of phenylalanine 100 μM for 16 h. The emission reaches 540 a.u after 48 h, a value that exceeds the intensities observed for both 100 μM and 200 μM and incubation times longer than 60 h. Thus, a higher phenylalanine concentration, self-assembly is faster and the violet fluorescence was

greater. It must be emphasized that after 192 hours of incubation, the emission intensity was 1091 a.u. and the emission maximum had been redshifted to 444 nm.

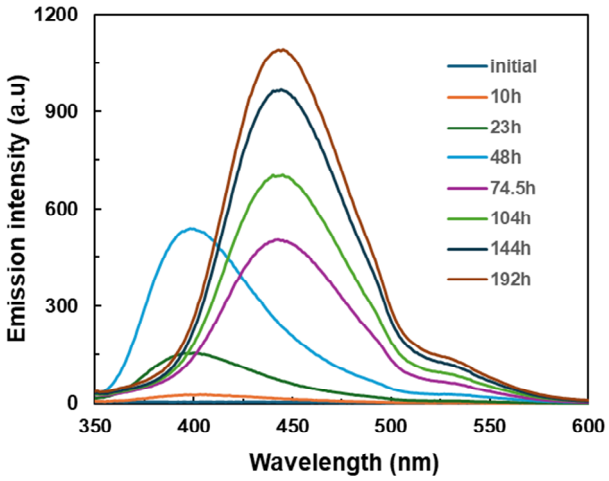

Figure 6. 2D emission spectra of phenylalanine (1 mM) prepared in 50 mM Tris buffer at pH 7.4. The spectra were recorded initially (blue) and after incubation for 10 h (orange), 23 h (green), 48 h (light blue), 74.5 h (magenta), 104 h (light green), 144 h (dark blue) and 192 h (dark orange) as a function of incubation time at 37 degrees.

The spontaneous self-assembly of phenylalanine and tyrosine was investigated at two different concentrations (1 mM and 100 μM) using two buffers by optical microscopy. At higher concentration (1 mM) there are evident fibrillar associations noticed before and after incubation for 20 h at 37 degrees (Figure 7, Panel A and B). These results are in the frame with previously reported data using FESEM and TEM techniques and samples in aqueous solutions.[24]

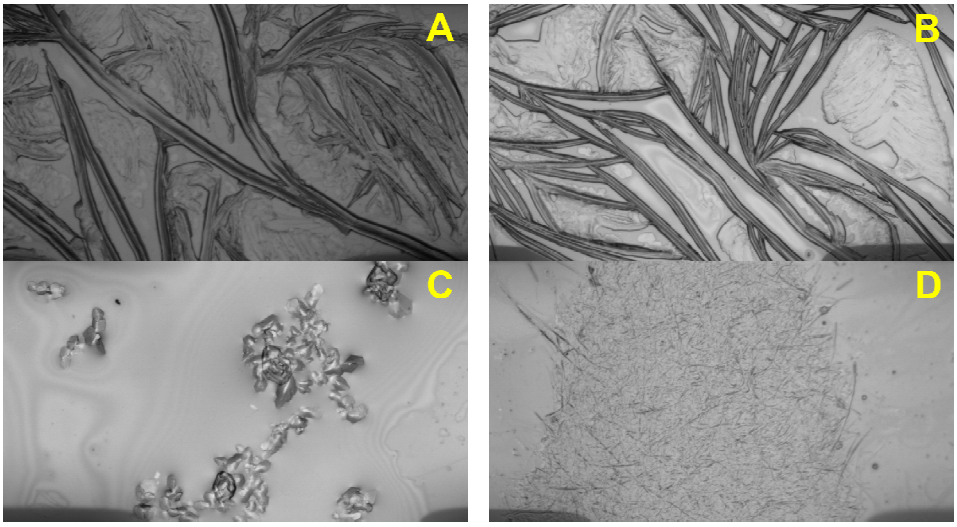

Figure 7. Images of phenylalanine samples originated from 1 mM and 100 µM solution prepared in Tris buffer 50 mM at pH 7.4 before (Panel A and C) and after incubation (Panel B and D) for 20 h at 37 degrees.

Additionally, phenylalanine crystal-like structures are seen at lower concentrations (100 µM; Figure 7, Panels C and D), and later, some little fibrils were seen. It's interesting to point out that the generated fibrils in phosphate buffer are thicker and congested at 1 mM, and following incubation, they often form more ordered supramolecular assemblies (Figure 8, Panel A). At lower concentrations, however, feather-like architecture occurred (Figure 8, Panel C), and thereafter incubation, the structure assembled as a spherulite (Figure 8, Panel D).

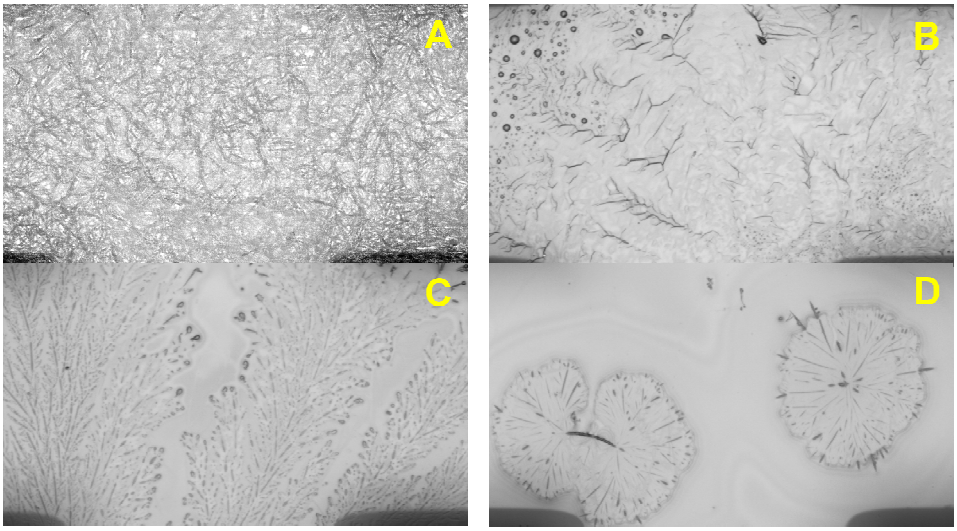

Figure 8. Images of phenylalanine samples originated from 1 mM and 100 µM solution prepared in phosphate buffer 50 mM at pH 7.4 before (Panel A and C) and after incubation (Panel B and D) for 20 h at 37 degrees.

The self-assembly of tyrosine was also investigated in similar conditions (Figures 9 and 10). Elongated isolated needles were observed at higher tyrosine concentration (1 mM) in Tris buffer (Figure 9, Panel A).

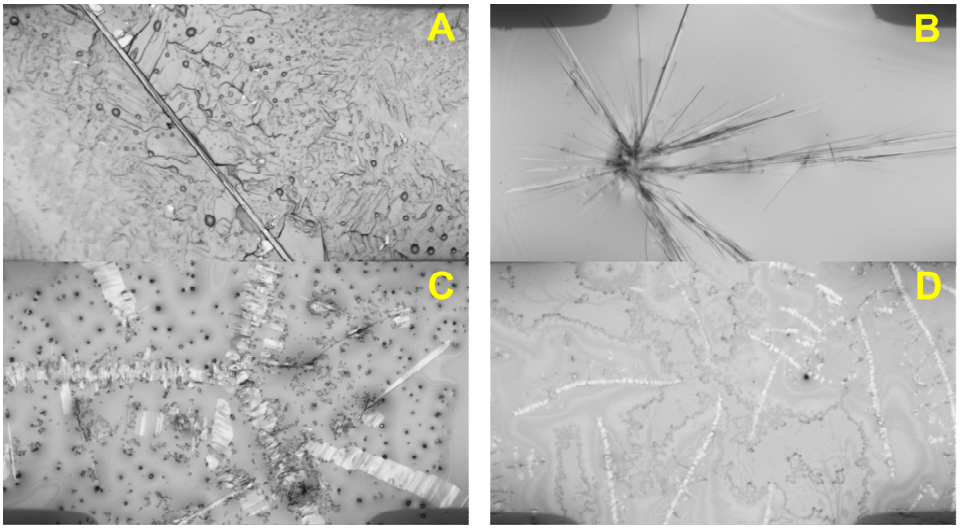

Figure 9. Images of tyrosine samples originated from 1 mM and 100 µM solution prepared in Tris buffer 50 mM at pH 7.4 before (Panel A and C) and after incubation (Panel B and D) for 20 h at 37 degrees.

Nucleation sites were identified as a starting point to the development of needles as fiber-shaped assemblies following incubation.

Similar self-assembly patterns were also reported for tyrosine in aqueous solutions.[21] The behavior was slightly different at low tyrosine concentrations. However, fibrillar lamella structure were initially remarked (Figure 9, Panel C). These become thinner after incubation (Figure 9, Panel D). In phosphate buffer the assembly was more difficult to fulfill. Thus, at lower amino acid concentration some fibrillar lamella were also distinguished, but after incubation these are not so well defined. Once again, the phosphate buffer seems to affect these initial well-organized patterns.

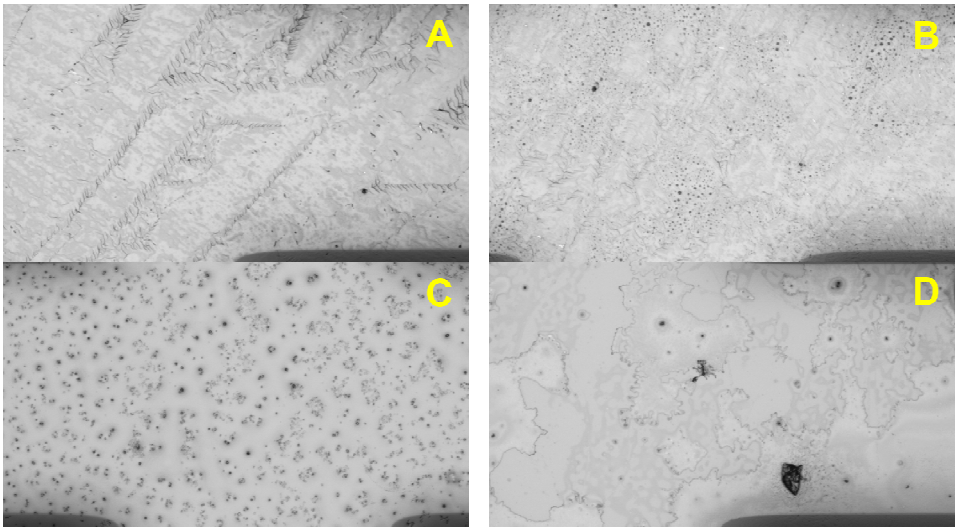

Figure 10. Images of tyrosine samples originated from 1 mM and 100 μM solution prepared in phosphate buffer 50 mM at pH 7.4 before (Panel A and C) and after incubation (Panel B and D) for 20 h at 37 degrees.

A similar trend was noticed at low amino acids concentration (Figure 8, Panels C and D; Figure 10, Panels C and D) in phosphate buffer. Generally, these images support our assumption that buffers also play an essential role in the self-assembling process. There is an open question that should be addressed: is Tris a promoter of amino acid self-assembling? Most probably

its hydroxylic groups might induce a network array that enhances self-assembly. Isothermal calorimetry has been used to demonstrate that Tris is enhancing binding of a cationic dye to a polyanion.[37] Another study demonstrates that a higher Tris concentration suppresses the aggregation of a thermal denatured bovine serum albumin.[38] Supplementary, tyrosine possesses a phenolic group that interplays in H bond interactions. Triggers that increase interparticle interactions are covered in a recent review.[39] Nevertheless, many challenges arise from the present study. Thus, many parameters should be considered when further studies will be engaged with emphasizing the physiological impact of these well-organizing supramolecular architectures.

Experimental

Chemicals and materials

L-Phenylalanine and L-tyrosine were purchased from Carl Roth GmbH, Karlsruhe, Germany. L-tryptophan were obtained from Merck, Darmstadt, Germany. Sodium phosphate dibasic dihydrate was from Steinheim, Germany and Tris from Carl Roth GmbH, Karlsruhe, Germany. All buffer and amino acid solutions were freshly prepared using ultrapure water (18.2 MΩ·cm, Millipore type, Milford, MA, USA) or a buffer and the pH value were adjusted using concentrated hydrochloric acid (1 M) and monitored using a Hannan pH-meter (Temse, Belgium). The amino acid samples were incubated at 37 degrees using a Termomixer (Eppendorf, Fisher Scientific).

UV-Vis and fluorescence spectroscopy

UV-Vis absorption spectra of diluted phenylalanine, tyrosine or tryptophane solutions were recorded in a 1 cm quartz cuvette (Hellma, Müllheim, Germany) using a Libra UV-Vis spectrophotometer (Biochrom,

Cambridge, UK). Each spectrum was recorded using a scan speed of 2649 nm/min (scan step 1 nm), in a spectral range of 200–400 nm. All amino acids were dissolved and diluted Tris buffer 0.1 M with a pH 7.4.

Before measuring the amino acids 3D spectra stock amino acid solutions (100 μM or 200 μM) were incubated at 37 degrees at different periods. After incubation the emission spectra of the phenylalanine samples were directly measured at room temperature (22 degrees).

Fluorescence spectra for each amino acid solution, placed into a four-side transparent quartz cuvette (maximum volume of 1.7 mL, Hellma, Müllheim, Germany), were measured on a JASCO FP-8350 Spectrofluorometer (Tokyo, Japan). 2D spectra were recorded in the emission range of 270-600 nm using a characteristic excitation wavelength for each amino acid (258 nm for phenylalanine; 275 nm for tyrosine and 279 nm for tryptophane) and a scanning speed of 1000 nm/min. All spectral measurements were made in triplicates. The blue 2D fluorescence spectra of concentrated phenylalanine (1 mM) samples were recorded in the emission range of 325-600 nm using an excitation wavelength of 315 nm and a scanning speed of 500 nm/min, number of five accumulation per spectrum.

3D fluorescence spectra were obtained using an excitation range 200–589 nm and an emission range 210–600 nm; $\Delta\lambda_{incr}$ = 10 nm, a scanning speed of 5000 nm/min, number of accumulation 3 and both inlet and outlet slits with 5 nm wide. The final volume of each sample was 1 mL. A blank 3D fluorescence spectrum was also taken in a similar fashion using a similar volume of buffer (Tris 50 mM pH 7.4) and automatically extracted during each acquisition. The time required for every 3D spectrum acquisition was around 2.5 h.

Microscopy studies

Two phenylalanine stock solutions (25-27 mM) were prepared in suitable buffer (Tris 50 mM or Phosphate 50 mM both with a pH 7.4). A

tyrosine stock solution (51 mM) was prepared using an alkaline solution (60 mM NaOH). Diluted solutions of phenylalanine or tyrosine (1 mM or 100 µM) were made in each buffer using concentrated solutions described above. After dilution 1 µL of each sample was transferred immediately to the glass slide and leave it to dry. Before this step, all slides were soaked in an alcoholic acidic solution (50 mL ethanol and 1 mL HCl 25%), and each one was rinsed three times with bidistilled water respectively ethanol and lately dried. The sample were incubated for 20 h at 37 degrees with continuous shaking at 300 rpm. After incubation a similar volume was placed onto a glass slide and dried. The buffers were also transferred to glass slides and investigated as controls.

Samples patterns observed after casting and drying on glass slides were assessed using a Malvern Morphologi G3SE optical characterization system (Malvern Instruments, Malvern, UK).

Conclusions

Findings from 2D and 3D fluorescence spectra analysis indicated that all aromatic amino acids have capacity of self-assembly and this process could be dynamically assessed in both UV and Vis spectral emission range at concentrations lower than 200 µM. Blue emission fluorescence signals were noticed at moderate incubation times (hours) when a phenylalanine concentration of 100 µM, closer to the physiological one, was used. Similar profiles were also obtained at 200 µM, with a faster signal in blue emission zone centered around 443 nm when two excitation wavelengths at 225 or 315 nm were used. In any case, violet fluorescence first appeared in the first two incubation days when concentration had arisen at 1 mM. At longer incubation times the fluorescence maximum shifts to

blue fluorescence. Self-assembly was also supported by classical microscopy. Both phenylalanine and tyrosine have a pronounced tendency to form well-organized structures especially in Tris buffer. Further work is needed to establish how different key factors such type of buffer, amino acid levels, presence of proteins, essential minerals or pH might have an impact on kinetics of self-assembly.

Acknowledgements

This scientific work was funded by UEFISCDI, grant number PN-III-P2-2.1-PED-2019-2484.

References

1. Yanari, S.; Bovey, F. A. Interpretation of the ultraviolet spectral changes of proteins. *J. Biol. Chem.* **1960**, *235*(10), 2818 – 2826. https://doi.org/10.1016/S0021-9258(18)64546-6
2. Metsämuuronen, S.; Mänttäri, M.; Nyström, M. Comparison of analysis methods for protein concentration and its use in UF fractionation of whey. *Desalination* **2011**, *283*, 156 – 164. https://doi.org/10.1016/j.desal.2011.02.012
3. Ghisaidoobe, A. B. T.; Chung, S. J. Intrinsic tryptophan fluorescence in the detection and analysis of proteins: A focus on förster resonance energy transfer techniques. *Int. J. Mol. Sci.* **2014**, *15*(12), 22518 – 22538. https://doi.org/10.3390/ijms151222518
4. Liu, Y.; Xu, J.; Han, L.; Liu, Q.; Yang, Y.; Li, Z.; Lu, Z.; Zhang, H.; Guo, T.; Liu, Q. Theoretical research on excited states: ultraviolet and fluorescence spectra of aromatic amino acids. *Interdiscip. Sci. Comput. Life Sci.* **2020**, *12*(4), 530 – 536. https://doi.org/10.1007/s12539-020-00395-3
5. Locquet, N.; Aït-Kaddour, A.; Cordella, C. B. Y. 3D Fluorescence Spectroscopy and its applications. In Encyclopedia of analytical chemistry, John Wiley & Sons: Portico, 2018, pp. 1 – 39. https://doi.org/10.1002/9780470027318.a9540
6. Christensen, J.; Nørgaard, L.; Bro, R., Engelsen, S. B. Multivariate autofluorescence of intact food systems. *Chem. Rev.* **2006**, *106*(6), 1979 – 1994. https://doi.org/10.1021/cr050019q

7. Rovelli, V.; Longo, N. Phenylketonuria and the brain. *Mol. Genet. Metab.* **2023**, *139*(1), 107583. https://doi.org/10.1016/j.ymgme.2023.107583

8. de Almeida Duarte, C. M.; Piazzon, F. B.; Rocco, I. S.; de Mello, C. B. Influence of blood phenylalanine level variations on the development of executive functions and social cognition in children with phenylketonuria. *J. Pediatr.* **2023**, *99*(5), 507 – 513. https://doi.org/10.1016/j.jped.2023.04.003

9. ten Hoedt, A. E.; de Sonneville, L. M.; Francois, B.; ter Horst, N. M.; Janssen, M. C.; Rubio-Gozalbo, M. E.; Wijburg, F. A.; Hollak, C. E.; Bosch, A. M. High phenylalanine levels directly affect mood and sustained attention in adults with phenylketonuria: a randomised, double-blind, placebo-controlled, crossover trial. *J. Inherit. Metab. Dis.* **2011**, *34*(1), 165 – 171. https://doi.org/10.1007/s10545-010-9253-9

10. Blau, N.; van Spronsen, F. J.; Levy, H. L. Phenylketonuria, *Lancet* **2010**, *376* (9750), 1417 – 1427. https://doi.org/10.1016/S0140-6736(10)60961-0

11. Adler-Abramovich, L.; Vaks, L.; Carny, O.; Trudler, D.; Magno, A.; Caflisch, A.; Frenkel, D.; Gazit, E. Phenylalanine assembly into toxic fibrils suggests amyloid etiology in phenylketonuria. *Nat. Chem. Biol.* **2012**, *8*(8), 701 – 706. https://doi.org/10.1038/nchembio.1002

12. Anand, B. G.; Dubey, K.; Shekhawat, D. S.; Kar, K. Intrinsic property of phenylalanine to trigger protein aggregation and hemolysis has a direct relevance to phenylketonuria. *Sci. Rep.* **2017**, *7*(1), 11146. https://doi.org/10.1038/s41598-017-10911-z

13. Szigetvari, P. D.; Patil, S.; Birkeland, E.; Kleppe, R.; Haavik, J. The effects of phenylalanine and tyrosine levels on dopamine production in rat PC12 cells. Implications for treatment of phenylketonuria, tyrosinemia type 1 and comorbid neurodevelopmental disorders. *Neurochem. Int.* **2023**, *171*, 105629. https://doi.org/10.1016/j.neuint.2023.105629

14. Morrow, G.; Tanguay, R. M. Biochemical and clinical aspects of hereditary tyrosinemia type 1. *Adv. Exp. Med. Biol.* **2017**, *959*, 9 – 21. https://doi.org/10.1007/978-3-319-55780-9_2

15. Nandy, T.; Biswas, R. Inhibition of amyloid fibrillation of single amino acid tryptophan by tannic acid: An insight into targeted therapy of hypertryptophanemia disorder, *Photochem. Photobiol. A Chem.* **2024**, *453*, 115660. https://doi.org/10.1016/j.jphotochem.2024.115660

16. Ferreira, P.; Shin, I.; Sosova, I.; Dornevil, K.; Jain, S.; Dewey, D.; Liu, F.; Liu, A. Hypertryptophanemia due to tryptophan 2,3-dioxygenase deficiency. *Mol. Genet. Metab.* **2017**, *120*(4), 317 – 324. https://doi.org/10.1016/j.ymgme.2017.02.009

17. Andrade, V. S.; Rojas, D. B.; Oliveira, L.; Nunes, M. L.; de Castro, F. L.; Garcia, C.; Gemelli, T.; de Andrade, R. B.; Wannmacher, C. M. Creatine and pyruvate prevent behavioral and oxidative stress alterations caused by hypertryptophanemia in rats. *Mol. Cell. Biochem.* **2012**, *362*(1–2), 225 – 232. https://doi.org/10.1007/s11010-011-1147-0

18. Cervenka, I.; Agudelo, L. Z.; Ruas, J. L. Kynurenines: Tryptophan's metabolites in exercise, inflammation, and mental health. *Science* **2017**, *357*(6349), eaaf9794. https://doi.org/10.1126/science.aaf9794

19. Tomar, D.; Chaudhary, S.; Jena, K. C. Self-assembly of L-phenylalanine amino acid: electrostatic induced hindrance of fibril formation. *RSC Adv.* **2019**, *9*(22), 12596 – 12605. https://doi.org/10.1039/C9RA00268E

20. Makhlynets, O. V.; Korendovych, I. V. A single amino acid enzyme. *Nat. Catal.* **2019**, *2*, 949 – 950. https://doi.org/10.1038/s41929-019-0379-3

21. Ménard-Moyon, C.; Venkatesh, V.; Krishna, K. V.; Bonachera, F.; Verma, S.; Bianco, A. Self-assembly of tyrosine into controlled supramolecular nanostructures. *Chemistry* **2015**, *21*(33), 11681 – 11686. https://doi.org/10.1002/chem.201502076

22. Zaguri, D.; Kreiser, T.; Shaham-Niv, S.; Gazit, E. Antibodies towards tyrosine amyloid-like fibrils allow toxicity modulation and cellular imaging of the assemblies. *Molecules* **2018**, *23*(6), 1273. https://doi.org/10.3390/molecules23061273

23. Singh, P.; Sharma, R. K.; Katare, O. P.; Wangoo, N. Understanding tyrosine self-assembly: from dimer assembly to magnetized fluorescent nanotubes embedded into PVA films. *Mater. Adv.* **2022**, *3*(16), 6518 – 6528. https://doi.org/10.1039/D2MA00546H

24. Banik, D.; Kundu, S.; Banerjee, P.; Dutta, R.; Sarkar, N. Investigation of fibril forming mechanisms of l-phenylalanine and l-tyrosine: Microscopic insight toward phenylketonuria and tyrosinemia type II. *J. Phys. Chem. B* **2017**, *121*(7), 1533 – 1543. https://doi.org/10.1021/acs.jpcb.6b12220

25. Prajapati, K. P.; Anard, B. G., Ansari, M.; Tiku, A. B.; Kar, K. Tryptophan self-assembly yields cytotoxic nanofibers containing amyloid-mimicking and cross-seeding competent conformers. *Nanoscale* **2022**, *14*, 16270-16285. https://doi.org/10.1039/D2NR03544H

26. Babar, D. G.; Sarkar, S. Self-assembled nanotubes from single fluorescent amino acid. **2017**, *Appl. Nanosci. 7*, 101 – 107. https://doi.org/10.1007/s13204-017-0551-5

27. Cardozo, G. C.; Duarte, E. L.; da Cunha, A. R.; Soga, D.; de Almeida Rizzutto, M., Lamy, M. T.; Milán-Garcés, E. A., Label-free detection of π-stacking interactions during tryptophan self-assembling into amyloid-like structures

using surface-enhanced Raman Scattering. *J. Raman Spectrosc.* **2025**, *56*(10) 987 – 998. https://doi.org/10.1002/jrs.6835

28. Kawabata, K.; Kanoh, M.; Okazaki, M.; Maeda, R. Mori, S.; Akimoto, S.; Inagaki, M., & Nishi, H. Photoprotective effects of selected amino acids on naproxen photodegradation in aqueous media. *Pharmaceuticals* **2020**, *13*(6), 135. https://doi.org/10.3390/ph13060135

29. Khemaissa, S; Walrant, A.; Sagan, S. Tryptophan, more than just an interfacial amino acid in the membrane activity of cationic cell-penetrating and antimicrobial peptides. *Q. Rev. Biophys.* **2022**, 55, e10. https://doi.org/10.1017/S0033583522000105

30. Uyaver, S. Tyrosine, phenylalanine, and tryptophan undergo self-aggregation in similar and different manners. *Atmosphere* **2022**, *13*(9), 1448. https://doi.org/10.3390/atmos13091448

31. Scholl-Buergi, S.; Neurauter, G.; Karall, D.; Fuchs, D. Serum phenylalanine concentrations in patients post trauma and burn correlate to neopterin concentrations. *J. Inherit. Metab. Dis.* **2009**, *32*, 587 – 588. https://doi.org/10.1007/s10545-009-9960-2

32. Clearya, M.; Trefz, F.; Muntau, A. C.; Feillet, F.; van Spronsen, F. J.; Burlina, A.; Bélanger-Quintana, A.; Giżewska, M.; Gasteygeri, C.; Bettiol, E.; Blau, N.; MacDonald, A. Fluctuations in phenylalanine concentrations in phenylketonuria: A review of possible relationships with outcomes *Mol. Genet. Metab*. **2013**, *110*(4), 418 – 423. https://doi.org/10.1016/j.ymgme.2013.09.001

33. Waisbren, S. E; Noel, K.; Fahrbach, K.; Cella, C.; Frame, D.; Dorenbaum, A.; Levy, H. Phenylalanine blood levels and clinical outcomes in phenylketonuria: a systematic literature review and meta-analysis. *Mol. Genet. Metab*. **2007**, *92*(1–2), 63 – 70. https://doi.org/10.1016/j.ymgme.2007.05.006

34. Bagchi, D.; Maity, A.; De, S. K.; Chakraborty, A. Effect of metal ions on the intrinsic blue fluorescence property and morphology of aromatic amino acid self-assembly. *J. Phys. Chem. B* **2021**, *125*(45), 12436 – 12445. https://doi.org/10.1021/acs.jpcb.1c07392

35. Liu, H. X.; Zhang, R. S.; Yao, X. J.; Liu, M. C.; Hu, Z. D.; Fan, B. T. Prediction of the isoelectric point of an amino acid based on GA-PLS and SVMs. *J. Chem. Inf. Comput. Sci.* **2004**, *44*(1), 161 – 167. https://doi.org/10.1021/ci034173u

36. Bortolotti, A.; Wong, Y. H.; Korsholm, S. S.; Bahring, N. H. B.; Bobone, S.; Tayyab, S.; van de Weert, M.; Stella, L. On the purported "backbone fluorescence" in protein three-dimensional fluorescence spectra. *RSC Adv.* **2016**, *6*(114), 112870 – 112876. https://doi.org/10.1039/C6RA23426G

37. Rodrigo, A. C; Laurini, E.; Vieira, V. M. P.; Pricl, S., & Smith, D. K. Effect of buffer at nanoscale molecular recognition interfaces – electrostatic binding of biological polyanions. *Chem. Commun.* **2017**, *53*(84), 11580 – 11583. https://doi.org/10.1039/C7CC07413A

38. Taha, M. and Lee, M.-J. Interactions of TRIS [tris(hydroxymethyl)-aminomethane] and related buffers with peptide backbone: Thermodynamic characterization. *Phys. Chem. Chem. Phys.* **2010**, *12*(39), 12840. https://doi.org/10.1039/c0cp00253d

39. Roy, S. and Pillai, P. P. What triggers the dynamic self-assembly of molecules and materials? *Langmuir* **2023**, *39*(37), 12967 – 12974. https://doi.org/10.1021/acs.langmuir.3c01142